Synthesis, Structure, and Bonding of the Unusual μ-σ,σ-Allenylidene Complex $[Rh_2(\mu\text{-}OOCCH_3)(\mu\text{-}\sigma,\sigma\text{-}C{=}C{=}CPh_2)(CO)_2(PCy_3)_2]BF_4$

Andrew J. Edwards, Miguel A. Esteruelas,* Fernando J. Lahoz, Javier Modrego, Luis A. Oro,* and Jörg Schrickel

Departamento de Química Inorgánica, Instituto de Ciencias de Materiales de Aragón, Universidad de Zaragoza, CSIC, 50009 Zaragoza, Spain

Received March 5, 1996[⊗]

The binuclear complex $[Rh(\mu\text{-}OOCCH_3)(CO)(PCy_3)]_2$ (**1**) reacts with 1,1-diphenyl-2-propyn-1-ol to give $[Rh_2(\mu\text{-}OOCCH_3)(\mu\text{-}\eta^1{:}\eta^2\text{-}C_2C(OH)R_2)(CO)_2(PCy_3)_2]$ (**2**), which affords $[Rh_2(\mu\text{-}OOCCH_3)(\mu\text{-}\sigma,\sigma\text{-}C{=}C{=}CPh_2)(CO)_2(PCy_3)_2]BF_4{\cdot}^1/_2CH_2Cl_2$ (**3**) by protonation with $HBF_4{\cdot}OEt_2$. The molecular structure of **3** can be described as a coordinatively unsaturated (30 valence electrons according to the EAN rule) dinuclear species, containing a single rhodium−rhodium bond (d(Rh−Rh) = 2.723(1) Å). Additionally, the metal centers are bridged by an allenylidene ligand and a carboxylate group. The $C_\alpha-C_\beta$ and $C_\beta-C_\gamma$ distances of the former are 1.30(1) and 1.32(1) Å, while the $C_\alpha-C_\beta-C_\gamma$ angle is 174.4(12)°. The electronic structure of the model cations $[Rh_2(\mu\text{-}OOCH)(\mu\text{-}\sigma,\sigma\text{-}C{=}C{=}CH_2)(CO)_2(PH_3)_2]^+$ (**5**) and $[Rh_2(\mu\text{-}OOCH)(\mu\text{-}C{=}CH_2)(CO)_2(PH_3)_2]^+$ (**6**) have been studied by means of approximate EHT MO calculations. The interaction of the vinylidene ligand with the bimetallic unit is similar to that of the allenylidene. For both cases the unsaturated η^1-carbon ligand has a net acceptor behavior. In the allenylidene ligand the highest negative charge is located on the C_α carbon atom; this charge decreases toward the C_γ carbon atom. In contrast, for the complex **6**, the C_α bridging carbon atom is the least negatively charged.

Introduction

Transition-metal vinylidene complexes, $M{=}C{=}CR_2$, have been the subject of intensive study in recent years. In contrast, the chemistry of the related allenylidene derivatives, $M{=}C{=}C{=}CR_2$, is less developed.[1] Although several synthetic routes have been described for the generation of the $M{=}C{=}C{=}CR_2$ unit,[2] the most versatile appears to involve terminal alkynols $HC{\equiv}CCR_2OH$ as starting materials.[3] From a mechanistic point of view, it has been proposed that, following alkyne coordination, a rearrangement occurs to give a CR_2OH-substituted vinylidene compound as an intermediate, which spontaneously dehydrates to form the final product.[3a,b]

The binuclear μ-σ,σ-allenylidene derivatives are rare. The complexes of this type previously reported are neutral species of 34 valence electrons of W,[4] Mn,[5,6] and Fe,[7,8] which have been prepared by some of the following methods: (i) thermal decomposition of mononuclear allenylidene compounds;[4] (ii) addition of $M(CO)_n$ fragments to mononuclear allenylidene complexes;[4,6] (iii) reactions of vinylidene-bridged complexes with tetracyanoethylene;[8] (iv) treatment of binuclear compounds containing the acetylenic dianion $^-C{\equiv}CC(O^-)^tBu_2$ with $COCl_2$.[5,7] Surprisingly, terminal alkynols have not been used to prepare the μ-σ,σ-allenylidene complexes.

We have previously reported the reaction of the binuclear complex $[Rh(\mu\text{-}OOCCH_3)(CO)(PCy_3)]_2$ with terminal alkynes $HC{\equiv}CR$ gives $[Rh_2(\mu\text{-}OOCCH_3)(\mu\text{-}\eta^1{:}\eta^2\text{-}C_2R)(CO)_2(PCy_3)_2]$ (R = Ph, CO_2CH_3, $SiMe_3$), where the asymmetric coordination of the alkynyl ligands was

[⊗] Abstract published in *Advance ACS Abstracts,* July 1, 1996.

(1) Bruce, M. I. *Chem. Rev.* **1991**, *91*, 197.
(2) (a) Fischer, E. O.; Kalder, H. J.; Köhler, F. H.; Huttner, G. *Angew. Chem., Int. Ed. Engl.* **1976**, *15*, 623. (b) Berke, H. *Chem. Ber.* **1980**, *113*, 1370. (c) Berke, H.; Härter, P.; Huttner, G.; Zsolnai, L. *Z. Naturforsch., B: Anorg. Chem., Org. Chem.* **1981**, *36*, 929. (d) Berke, H.; Huttner, G.; von Seyerl, J. *Z. Naturforsch., B: Anorg. Chem., Org. Chem.* **1981**, *36*, 1277. (e) Berke, H.; Härter, P.; Huttner, G.; von Seyerl, J. *J. Organomet. Chem.* **1981**, *219*, 317. (f) Kolobova, N. E.; Ivanov, L. L.; Zhvanko, O. S.; Checkulina, I. N.; Derunov, V. V. *Izv. Akad. Nauk SSSR, Ser. Khim.* **1982**, 2632. (g) Binger, P.; Müller, P.; Wenz, R.; Mynott, R. *Angew. Chem., Int. Ed. Engl.* **1990**, *29*, 1037. (h) Deutsch, M.; Stein, F.; Lackmann, R.; Pohl, E.; Herbst-Irmer, R.; de Meijere, A. *Chem. Ber.* **1992**, *125*, 2051.
(3) (a) Selegue, J. P. *Organometallics* **1982**, *1*, 217. (b) Selegue, J. P. *J. Am. Chem. Soc.* **1983**, *105*, 5921. (c) Le Bozec, H.; Ouzzine, K.; Dixneuf, P. H. *J. Chem. Soc., Chem. Commun.* **1989**, 219. (d) Selegue, J. P.; Young, B. A.; Logan, S. L. *Organometallics* **1991**, *10*, 1972. (e) Wolinska, A.; Touchard, D.; Dixneuf, P. H.; Romero, A. *J. Organomet. Chem.* **1991**, *420*, 217. (f) Pirio, N.; Touchard, D.; Toupet, L.; Dixneuf, P. H. *J. Chem. Soc., Chem. Commun.* **1991**, 980. (g) Pilette, D.; Ouzzine, K.; Le Bozec, H.; Dixneuf, P. H.; Rickard, C. E. F.; Roper, W. R. *Organometallics* **1992**, *11*, 809. (h) Lomprey, J. R.; Selegue, J. P. *Organometallics* **1993**, *12*, 616. (i) Pirio, N.; Touchard, D.; Dixneuf, P. H. *J. Organomet. Chem.* **1993**, *462*, C18. (j) Schwab, P.; Werner, H. *J. Chem. Soc., Dalton Trans.* **1994**, 3415. (k) Cadierno, V.; Gamasa, M. P.; Gimeno, J.; Borge, J.; Garcia-Granda, S. *J. Chem. Soc., Chem. Commun.* **1994**, 2495. (l) Cadierno, V.; Gamasa, M. P.; Gimeno, J.; Lastra, E.; Borge, J.; Garcia-Granda, S. *Organometallics* **1994**, *13*, 745. (m) Werner, H.; Rappert, T.; Wiedemann, R.; Wolf, J.; Mahr, N. *Organometallics* **1994**, *13*, 2721. (n) Cadierno, V.; Gamasa, M. P.; Gimeno, J.; Lastra, E. *J. Organomet. Chem.* **1994**, *474*, C27. (o) Touchard, D.; Pirio, N.; Dixneuf, P. H. *Organometallics* **1995**, *14*, 4920. (p) Werner, H.; Stark, A.; Steinert, P.; Grünwald, C.; Wolf, J. *Chem. Ber.* **1995**, *128*, 49. (q) Peron, D.; Romero, A.; Dixneuf, P. H. *Organometallics* **1995**, *14*, 3319. (r) Braun, T.; Steinert, P.; Werner, H. *J. Organomet. Chem.* **1995**, *488*, 169.
(4) Berke, H.; Härter, P.; Huttner, G.; Zsolnai, L. *Chem. Ber.* **1982**, *115*, 695.
(5) Berke, H.; Härter, P.; Huttner, G.; Zsolnai, L. *Chem. Ber.* **1984**, *117*, 3423.
(6) Kolobova, N. E.; Ivanov, L. L.; Zhvanko, O. S.; Aleksandrov, G. G.; Struchkov, Yu. T. *J. Organomet. Chem.* **1982**, *228*, 265.
(7) Berke, H.; Grössmann, U.; Huttner, G.; Zsolnai, L. *Chem. Ber.* **1984**, *117*, 3432.
(8) (a) Etienne, M.; Toupet, L. *J. Chem. Soc., Chem. Commun.* **1989**, 1110. (b) Etienne, M.; Talarmin, J.; Toupet, L. *Organometallics* **1992**, *11*, 2058.

S0276-7333(96)00164-1 CCC: $12.00

Scheme 1

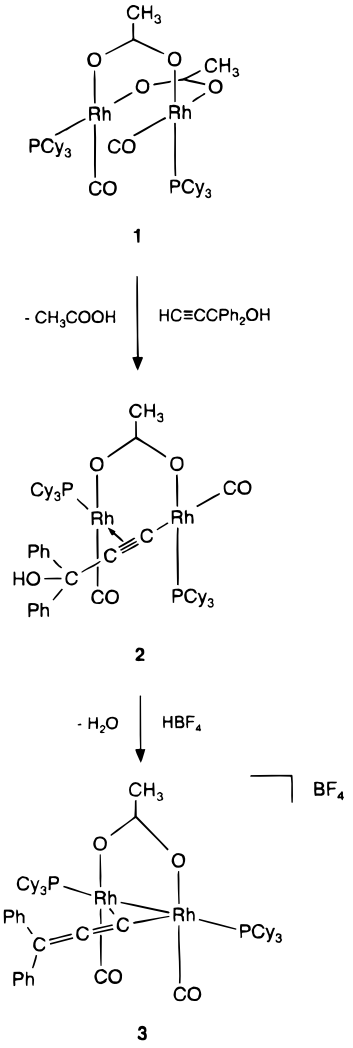

established by an X-ray investigation on a monocrystal of $[Rh_2(\mu\text{-}OOCCH_3)(\mu\text{-}\eta^1{:}\eta^2\text{-}C_2Ph)(CO)_2(PCy_3)_2]$.[9] The protonation of these compounds with $HBF_4{\cdot}OEt_2$ affords the corresponding vinylidene-bridged rhodium derivatives $[Rh_2(\mu\text{-}OOCCH_3)(\mu\text{-}C{=}CHR)(CO)_2(PCy_3)_2]^+$, which are the first examples of cationic vinylidene-bridged derivatives, and homobinuclear vinylidene-bridged compounds with 30 valence electrons.[10] The same reaction with disubstituted terminal alkynol should afford the related $\mu\text{-}\sigma,\sigma$-allenylidene derivative; we have thus carried out the reaction with 1,1-diphenyl-2-propyn-1-ol.

We report the synthesis, X-ray characterization, and comparative EHT-MO calculations of the unusual $\mu\text{-}\sigma,\sigma$-allenylidene derivative $[Rh_2(\mu\text{-}OOCCH_3)(\mu\text{-}\sigma,\sigma\text{-}C{=}C{=}CPh_2)(CO)_2(PCy_3)_2]^+$, which is the first cationic, unsaturated (30 valence electrons according to EAN), and group nine $\mu\text{-}\sigma,\sigma$-allenylidene complex.

Results and Discussion

Preparation of $[Rh_2(\mu\text{-}OOCCH_3)(\mu\text{-}\sigma,\sigma\text{-}C{=}C{=}CPh_2)(CO)_2(PCy_3)_2]BF_4$. Similarly to the reactions of the binuclear complex $[Rh(\mu\text{-}OOCCH_3)(CO)(PCy_3)]_2$ (**1**) with phenylacetylene, methyl propiolate, and (trimethyl)silylacetylene to give $[Rh_2(\mu\text{-}OOCCH_3)(\mu\text{-}\eta^1{:}\eta^2\text{-}C_2R)(CO)_2(PCy_3)_2]$ (R = Ph, CO_2CH_3, $SiMe_3$), the treatment of **1** with 1.1 equiv of 1,1-diphenyl-2-propyn-1-ol in hexane at room temperature leads to the derivative $[Rh_2(\mu\text{-}OOCCH_3)(\mu\text{-}\eta^1{:}\eta^2\text{-}C_2C(OH)Ph_2)(CO)_2(PCy_3)_2]$ (**2**, Scheme 1), which was isolated as a green solid in 82% yield.

The presence of the alkynyl ligand was established from the $^{13}C\{^1H\}$ NMR spectrum in chloroform-d_1, which shows two resonances corresponding to the acetylenic carbon atoms at about 111 and 99 ppm and a singlet at 76.1 ppm due to the $-C(OH)Ph_2$ carbon atom. Interestingly, the $^{31}P\{^1H\}$ NMR spectrum exhibits a doublet at 44.1 ppm with a Rh−P coupling constant of 147 Hz, suggesting a rapid oscillation of the alkynyl group between the two metal atoms in solution. As found for the related $[Rh_2(\mu\text{-}OOCCH_3)(\mu\text{-}\eta^1{:}\eta^2\text{-}C_2R)(CO)_2(PCy_3)_2]$ (R = Ph, CO_2CH_3, $SiMe_3$) complexes, the motion is still rapid at −60°C. The dynamic oscillation process of these alkynyl groups between the two rhodium atoms most probably involves a symmetrical $Rh_2(\mu\text{-}\eta^1\text{-}C_2R)$ bonding mode. An EHT-MO calculation on the fluxional movement in the model compound $[Rh_2(\mu\text{-}OOCH)(\mu\text{-}\eta^1{:}\eta^2\text{-}C_2H)(CO)_2(PH_3)_2]$ shows that the process has a low activation barrier, ca. 11.53 kcal·mol^{-1} at the EHT level.[9]

The addition of 1 equiv of $HBF_4{\cdot}OEt_2$ to a diethyl ether solution of **2** affords a violet solid from which a crystalline solid analyzing for $[Rh_2(\mu\text{-}OOCCH_3)(\mu\text{-}\sigma,\sigma\text{-}C{=}C{=}CPh_2)(CO)_2(PCy_3)_2]BF_4{\cdot}{}^1/_2CH_2Cl_2$ (**3**) was isolated in 78% yield after crystallization from dichloromethane−diethyl ether. From a mechanistic point of view the $\mu\text{-}\sigma,\sigma$-allenylidene complex **3** is most probably the result of the spontaneous dehydration of a hydroxyvinylidene-bridged intermediate, which is generated by electrophilic attack of the proton of the acid to the C_β carbon atom of alkynyl **2** (eq 1).

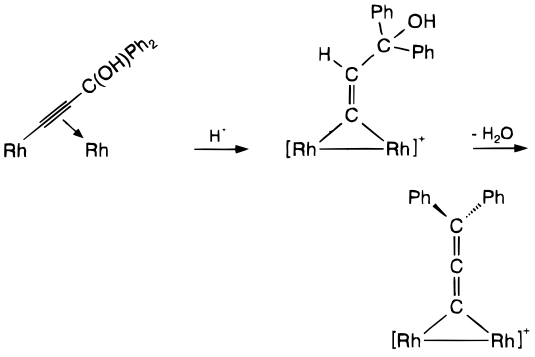

(1)

$Rh_2 = [Rh_2(\mu\text{-}OOCCH_3)(CO)_2(PCy_3)_2]$

The IR spectrum of **3** in Nujol exhibits two ν(CO) bands at 2026 and 1995 cm^{-1} as well as the ν_{asym}(OCO) (1538 cm^{-1}) and ν_{sym}(OCO) (1440 cm^{-1}) absorptions corresponding to the carboxylate group, which are separated by 98 cm^{-1}, in agreement with the bridging bidentate coordination mode of this ligand.[11] The most

(9) Esteruelas, M. A.; Lahuerta, O.; Modrego, J.; Nürnberg, O.; Oro, L. A.; Rodriguez, L.; Sola, E.; Werner, H. *Organometallics* **1993**, *12*, 266.

(10) Esteruelas, M. A.; Lahoz, F. J.; Oñate, E.; Oro, L. A.; Rodriguez, L.; *Organometallics* **1993**, *12*, 4219.

(11) (a) Mitchell, R. W.; Ruddick, J. D.; Wilkinson, G. J. *J. Chem. Soc. A* **1971**, 3224. (b) Robinson, S. D.; Uttley, M. F. *J. Chem. Soc., Dalton Trans.* **1973**, 1912. (c) Deacon, G. B.; Phillips, R. J. *Coord. Chem. Rev.* **1980**, *33*, 327. (d) Lahoz, F. J.; Martin, A.; Esteruelas, M. A.; Sola, E.; Serrano, J. L.; Oro, L. A. *Organometallics* **1991**, *10*, 1794.

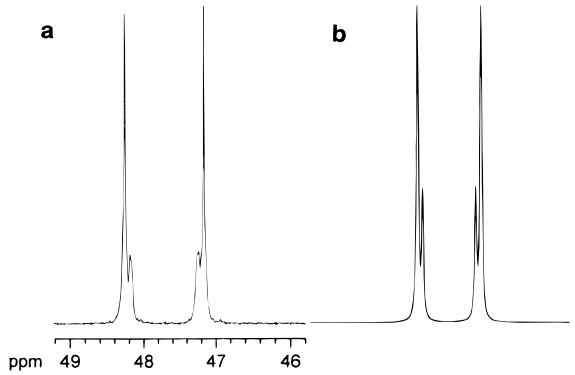

Figure 1. (a) observed $^{31}P\{^1H\}$ NMR ($CDCl_3$) spectrum of $[Rh_2(\mu\text{-}OOCCH_3)(\mu\text{-}\sigma,\sigma\text{-}C{=}C{=}CPh_2)(CO)_2(PCy_3)_2]BF_4$ (**3**). (b) Simulated spectrum (AA′XX′ system, A = P, X = Rh; $J_{P-P'} = 9$ Hz, $J_{P-Rh} = 134$ Hz, $J_{P-Rh'} = 116$ Hz).

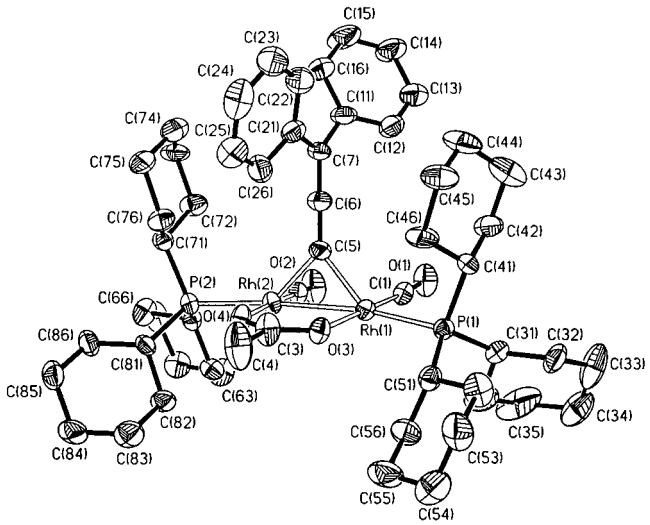

Figure 2. Molecular diagram of $[Rh_2(\mu\text{-}OOCCH_3)(\mu\text{-}\sigma,\sigma\text{-}C{=}C{=}CPh_2)(CO)_2(PCy_3)_2]^+$ (**3**), with 50% thermal ellipsoids shown.

interesting feature of this spectrum is the presence of a strong band at 1914 cm^{-1}. This absorption is attributed to the vibration of the allene bridging ligand and is also observed in the other μ-σ,σ-allenylidene complexes,[4−8] as well as in mononuclear allenylidene compounds.[1] We note that frequencies are higher for mononuclear complexes (between 1920 and 1961 cm^{-1}) than for the bimetallic derivatives (between 1835 and 1914 cm^{-1}). In addition, the absorption due to the $[BF_4]^-$ anion with T_d symmetry, centered at 1054 cm^{-1}, indicates that, although the metallic centers of **3** are coordinatively unsaturated, the anion is not coordinated to the rhodium atoms. In the $^{13}C\{^1H\}$ NMR spectrum the C_α carbon atom of the unsaturated η^1-carbon ligand is observed at 174.2 ppm as a triplet of triplets due to coupling with the rhodium ($J_{Rh-C} = 52$ Hz) and the phosphorus ($J_{P-C} = 36$ Hz) atoms. The C_β carbon atom gives a non-phosphorus-coupled resonance and, therefore, appears as a triplet at 181.34 ppm with a Rh−C coupling constant of 6 Hz, while the C_γ carbon atom gives rise to a singlet at 134.2 ppm. The $^{31}P\{^1H\}$ NMR spectrum, shown in Figure 1a, can be simulated using an AA′XX′ (A = P, X = Rh) system (Figure 1b) with $J_{A-A'} = 9$ Hz, $J_{A-X} = 134$ Hz, and $J_{A-X'} = 116$ Hz.

X-ray Structure of 3. Figure 2 shows the molecular structure of **3**. Selected bond distances and angles are listed in Table 1.

Table 1. Selected Bond Distances (Å) and Angles (deg) for Complex 3

Rh(1)−Rh(2)	2.723(1)	C(3)−C(4)	1.51(2)
Rh(1)−P(1)	2.364(2)	Rh(2)−P(2)	2.369(2)
Rh(1)−C(1)	1.799(10)	Rh(2)−C(2)	1.838(11)
Rh(1)−C(5)	1.988(10)	Rh(2)−C(5)	1.997(10)
Rh(1)−O(3)	2.082(7)	Rh(2)−O(4)	2.080(7)
C(5)−C(6)	1.30(1)	C(6)−C(7)	1.32(1)
C(7)−C(11)	1.47(2)	C(7)−C(21)	1.49(2)
O(3)−C(3)	1.28(1)	O(4)−C(3)	1.24(1)
C(1)−O(1)	1.17(1)	C(2)−O(2)	1.14(1)
Rh(1)−C(5)−Rh(2)	86.2(4)	C(5)−C(6)−C(7)	174.4(12)
P(1)−Rh(1)−Rh(2)	169.38(7)	P(2)−Rh(2)−Rh(1)	171.99(7)
O(3)−Rh(1)−Rh(2)	82.6(2)	O(4)−Rh(2)−Rh(1)	83.9(2)
C(1)−Rh(1)−Rh(2)	98.7(3)	C(2)−Rh(2)−Rh(1)	95.9(3)
C(5)−Rh(1)−Rh(2)	47.0(3)	C(5)−Rh(2)−Rh(1)	46.8(3)
P(1)−Rh(1)−C(5)	139.6(3)	P(2)−Rh(2)−C(5)	136.7(3)
P(1)−Rh(1)−O(3)	88.3(2)	P(2)−Rh(2)−O(4)	88.6(2)
P(1)−Rh(1)−C(1)	90.4(3)	P(2)−Rh(2)−C(2)	91.4(3)
O(3)−Rh(1)−C(1)	178.7(3)	O(4)−Rh(2)−C(2)	176.7(4)
Rh(1)−C(5)−C(6)	135.4(8)	Rh(2)−C(5)−C(6)	137.2(8)
Rh(1)−O(3)−C(3)	123.9(6)	Rh(2)−O(4)−C(3)	123.4(7)
O(3)−C(3)−C(4)	115.1(10)	O(4)−C(3)−C(4)	118.8(10)
O(3)−C(3)−O(4)	125.9(10)	C(11)−C(7)−C(21)	121.1(9)
C(6)−C(7)−C(11)	118.6(10)	C(6)−C(7)−C(21)	120.3(10)

The cation can be described as a dinuclear species of 30 valence electrons, containing a single rhodium−rhodium bond bridged by an allenylidene and an carboxylate ligand. Each rhodium is five coordinate and completes its coordination with one terminal phosphine and one carbonyl group. Four of the five atoms directly bonding each metal form a slightly distorted square planar geometry, while the fifth (C(5) from the allenylidene ligand) is located approximately 1.45(1) Å outside the plane. The atoms P(1), C(1), Rh(2), and O(3), thus, describe the square planar environment around the Rh(1) atom, with P(1) trans disposed to Rh(2) (P(1)−Rh(1)−Rh(2) = 169.38(7)°). Meanwhile, P(2), C(2), Rh(1), and O(4) form the square planar environment around Rh(2), with P(2) trans disposed to Rh(1) (P(2)−Rh(2)−Rh(1) = 171.99(7)°). The C_α carbon atom of the allene ligand (C5) is symmetrically bonded to both metals with Rh−C distances of 1.998(10) and 1.997(10) Å, similar to the related bond lengths in the vinylidene-bridged cation $[Rh_2(\mu\text{-}OOCCH_3)(\mu\text{-}C{=}CHPh)(CO)_2(PCy_3)_2]^+$ (**4**, 1.984(5) and 2.015(5) Å).[10] The Rh_2−μ-C plane is roughly perpendicular to the $(C_{ipso})_2$−C plane (87.5(2)°), while the Rh(1)−C(5)−Rh(2) angle (86.2(4)°) agrees well with the related vinylidene-bridged ligand in **4** (83.2(2)°)[10] and the carbonyl-bridged ligands in $[Rh_4(\mu\text{-}OOCCH_3)_4(\mu\text{-}CO)_4(CO)_4(NC_5H_4CH{=}NC_6H_4\text{-}OC_{14}H_{29})_4]$ (84.6(3) and 85.1(3)°).[11d] The symmetric disposition of the allenylidene ligand leads to statistically identical rhodium−phosphine, rhodium−carbonyl, and rhodium−carboxylate bond lengths (see Table 1). This is in contrast with that observed for **4**, where the asymmetry of the unsaturated η^1-carbon ligand produces two significantly different Rh−P distances (2.396(1) and 2.329(1) Å) and Rh−Rh−P bond angles (171.99(4)° and 139.30(4)°). The allenylidene ligand is almost linear (C(5)−C(6)−C(7) = 174.4(12)°, while the C_α−C_β distance (C(5)−C(6) = 1.30(1) Å) is statistically identical with the C_β−C_γ bond length (C(6)−C(7) = 1.32(1) Å), which agree well with average carbon−carbon bond lengths for a carbon−carbon double bond (1.32(1) Å).[12]

(12) Orpen, A. G.; Brammer, L.; Allen, F. H.; Kennard, O.; Taylor, R. *J. Chem. Soc., Dalton Trans.* **1989**, S1.

Finally, the Rh−Rh distance (2.723(1) Å) lies in the region to invoke a single metal−metal bond, slightly longer than that found in the related vinylidene-bridged cation $[Rh_2(\mu\text{-}OOCCH_3)(\mu\text{-}C{=}CHPh)(CO)_2(PCy_3)_2]^+$ (**4**; 2.6557(5) Å)[10] and in the complexes $[Rh_2(\eta^5\text{-}C_5H_5)\{\mu\text{-}\eta^4\text{-}C_4(CF_3)_2H^tBuCO\}(\mu\text{-}C{=}CH^tBu)]$ (2.625(2) Å),[13] $[Rh_2(\eta^5\text{-}C_9H_7)_2(\mu\text{-}C{=}CH_2(CO)_2]$ (2.691(1) Å),[14] and $[Rh_2(\eta^5\text{-}C_5H_5)(\mu\text{-}C{=}CH_3)_2(CO)_2]$ (2.684(0) Å).[15]

EHT-MO Calculations for 3. A study of the bonding in the allenylidene and vinylidene complexes was carried out due to the complexity of the interactions involving these ligands within the respective rhodium complexes. The electronic structure of complex **3** has been studied by means of approximate EHT-MO[16] calculations using the model compound $[Rh_2(\mu\text{-}OOCH)(\mu\text{-}\sigma,\sigma\text{-}C{=}C{=}CH_2)(CO)_2(PH_3)_2]^+$ (**5**). These results are compared with calculations for the model vinylidene complex $[Rh_2(\mu\text{-}OOCH)(\mu\text{-}C{=}CH_2)(CO)_2(PH_3)_2]^+$ (**6**) (which represents the bent compound $[Rh_2(\mu\text{-}OOCCH_3)(\mu\text{-}C{=}CHPh)(CO)_2(PCy_3)_2]^+$ (**4**) and the linear complex $[Rh_2(\mu\text{-}OOCCH_3)(\mu\text{-}C{=}CH_2)(CO)_2(PCy_3)_2]^+$ (**7**)[10]). General studies on the bonding of mononuclear vinylidene and allenylidene complexes have previously been published.[17]

The electronic structure of the binuclear fragment $[Rh_2(\mu\text{-}OOCH)(CO)_2(PH_3)_2]^+$ is shown in Figure 3a. Its orbital scheme is related to the interaction of two planar ML_3 units with some mixing among the d orbitals, due to the lower symmetry of the rhodium environment in the binuclear fragment compared with an ideal square planar geometry.[18] The occupied orbitals correspond to pairs of bonding and antibonding interactions between the d orbitals of each metallic atom; this leads to a formal bond order of zero between both metal atoms, consistent with a reduced overlap population of only 0.05 electrons between the rhodium atoms. The 10 d orbitals are populated by a total of 16 electrons; thus, the LUMO could act as the possible acceptor on the addition of the two remaining electrons donated by the interacting allene fragments. The fragment orbital energy levels for the ligand $\mu\text{-}\sigma,\sigma\text{-}C{=}C{=}CH_2$ are presented in Figure 3b.

Interaction between the bimetallic and the ligand fragments involves the orbital 6a′ (Figure 4a), which acts as a σ donor. This orbital overlaps with the 19a′ (empty) and 16a′ (occupied) fragment orbitals of the bimetallic moiety forming a typical three-center−four-electron interaction which, according to a Mülliken analysis, transfers 0.47 electrons from the organic ligand to the binuclear fragment. In addition, orbital 2a″ of the ligand (Figure 4b) acts as a π acceptor of 0.9 electrons from the binuclear fragment. The Mülliken analysis of the fragment electron population shows a net acceptor behavior for the ligand, with a total charge transfer of 0.32 electrons from the binuclear fragment to the organic ligand. Table 2 shows the distribution of partial charges among the C atoms of the ligand and their valence orbitals. The largest negative charge is located on the C_α atom, decreasing toward the C_γ atom. The partial population change on the s and p_y orbitals

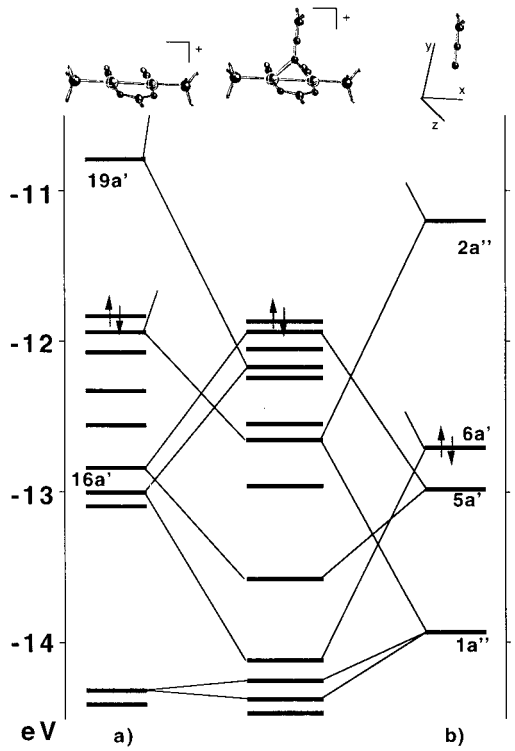

Figure 3. Molecular orbital diagram of complex $[Rh_2(\mu\text{-}OOCH)(\mu\text{-}\sigma,\sigma\text{-}C{=}C{=}CH_2)(CO)_2(PH_3)_2]^+$ (**5**) (center) showing the interaction of ligand $C{=}C{=}CH_2$ (a) with fragment $[Rh_2(\mu\text{-}OOCH)(CO)_2(PH_3)_2]^+$ (b).

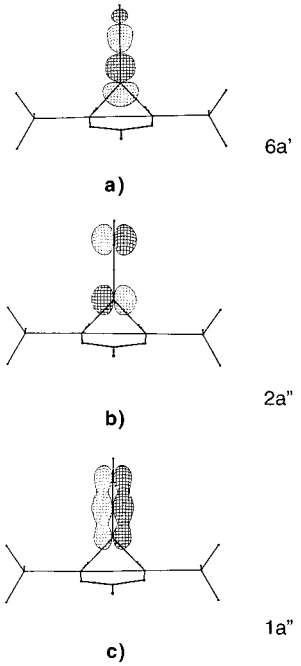

Figure 4. Some of the fragment orbitals of ligand $\mu\text{-}\sigma,\sigma\text{-}C{=}C{=}CH_2$ in model complex $[Rh_2(\mu\text{-}OOCH)(\mu\text{-}\sigma,\sigma\text{-}C{=}C{=}CH_2)(CO)_2(PH_3)_2]^+$ (**5**): σ donor 6a′ (a); π acceptor 2a″ (b); the fully π bonding combination of carbon p_x orbitals 1a″ (c).

(13) Dickson, R. S.; Fallon, G. D.; Mehere, F. I.; Nesbit, R. J. *Organometallics* **1987**, *6*, 215.
(14) Al-Obaidi, Y. N.; Green, M.; White, N. D.; Taylor, G. E. *J. Chem. Soc., Dalton Trans.* **1982**, 319.
(15) Herrmann, W. A.; Weber, C.; Ziegler, M. L.; Serhadli, O. *J. Organomet. Chem.* **1985**, *297*, 245.
(16) (a) Hoffmann, R. *J. Chem. Phys.* **1963,** *39*, 1397. (b) Hoffmann, R.; Lipscomb, W. N. *J. Chem. Phys.* **1962,** *36*, 3179. (c) Hoffmann, R.; Lipscomb, W. N. *J. Chem. Phys.* **1962,** *37*, 2872.
(17) (a) Stegmann, R.; Neuhaus, A.; Frenking, G. *J. Am. Chem. Soc.* **1993**, *115*, 11930. (b) Silvestr, J.; Hoffmann, R. *Helv. Chim . Acta* **1985,** *68*, 1461. (c) Kostic, N. M.; Fenske, R. F. *Organometallics* **1982**, *1*, 974. (d) Schilling, B. E. R.; Hoffmann, R.; Lichtenberger, D. L. *J. Am. Chem. Soc.* **1979**, *101*, 585.
(18) Albright, T. A.; Burdett, J. K.; Whangbo M. H. *Orbital Interactions in Chemistry*; John Wiley & Sons: New York, 1985.

Table 2. Distribution of Charge on the Carbon Atoms of the Allenylidene and Vinylidene Ligands in Model Complexes 5 and 6 and in the Fragments (in Parentheses)

ligand	C atom	tot charge (e^-)	S orbital	p_x	p_y	p_z
allenylidene	C_α	−0.196 (−0.656)	1.34 (1.51)	0.86 (0.51)	0.99 (1.50)	1.00 (1.13)
	C_β	−0.133 (0.101)	1.17 (1.16)	0.96 (0.98)	0.89 (0.86)	1.12 (0.91)
	C_γ	−0.096 (0.424)	1.19 (1.19)	1.04 (0.51)	0.95 (0.96)	0.92 (0.92)
vinylidne	C_α	−0.07 (−0.21)	1.35 (1.52)	0.81 (0.16)	1.01 (1.53)	0.90 (1.00)
	C_β	−0.30 (−0.02)	1.20 (1.19)	0.92 (0.91)	0.96 (0.93)	1.23 (1.00)

of the C_α atom upon coordination reflects the role of these orbitals as σ donors in the sp hybrid orbital 6a′. The variation on the partial population on the p_x orbital of the C_α and C_γ atoms clearly shows its π acceptor capability.

The electron donation from the ligand into acceptor orbital 19a′ of fragment $[Rh_2(\mu\text{-OOCH})(CO)_2(PH_3)_2]^+$ populates this metal−metal bonding combination of d orbitals whereas the corresponding antibonding combination remains empty, leading to a formal bond order of one between the metal atoms, as suggested from the X-ray crystal structure analysis. The final reduced orbital population between the rhodium atoms is 0.16 electrons. The group of 10 d orbitals in complex **5** are now formally populated by a total of 18 electrons. However, the bonding and antibonding combinations of the p_y orbitals of the rhodium atoms remain empty and are not involved in bonding, a result of the unsaturated coordination of these atoms. This allows rationalization of a 30 valence electron count, in accord with the EAN rule, since only 15 of the 18 available metal valence orbitals have electron density and are involved in bonding.

It is interesting to compare the bonding characteristics of the allenylidene **5** with those of the related vinylidene **6**. Thus, we have carried out a set of MO calculations on the model complex $[Rh_2(\mu\text{-OOCH})(\mu\text{-C=CH}_2)(CO)_2(PH_3)_2]^+$ (**6**). The interaction of the vinylidene ligand with the binuclear moiety is similar to that of the allenylidene (Figure 5). The main bonding interaction between the organic ligand and the binuclear fragment is a three-center−four-electron σ interaction between what is basically a ligand carbon sp hybrid orbital (4a′, Figure 6a) and the 19a′ (empty) and 16a′ (occupied) orbitals of the bimetallic unit. Furthermore there is a π acceptor interaction which transfers 0.8 electrons from the binuclear fragment to orbital 2a″ (Figure 6b) of the ligand. The total interaction is also very similar to the case of the allene ligand, leading to a net charge transfer of 0.25 electrons to the vinylidene ligand. As in the case of the allenylidene complex, the analysis of the reduced overlap population between the rhodium atoms shows an increase upon coordination of the organic bridge, from 0.06 electrons in the fragment to 0.16 electrons in the complex.

The difference in the charge distribution over the C atoms of both ligands in the model complexes **5** and **6** is significant as shown in Table 2. In the case of the vinylidene complex, the C_α bridging carbon atom is the least negative position of the organic ligand, whereas in the allenylidene bridge the C_α atom carries the most negative charge. As inferred from Table 2, this difference results from the role of the orbitals p_x in their respective fragments. In the vinylidene ligand the C_α p_x orbital takes part only in the π acceptor LUMO on coordination to the metals, while, the C_α p_x orbital in the allenylidene ligand is partially occupied in the free fragment, because it is involved in the π bonding combination 1a″ (Figure 4c). This significant amount of charge is incremented through back-donation from the binuclear moiety following coordination.

In contrast to the essentially linear complexes **3** and **7**, complex **4** is distorted and possesses one nonlinear P−Rh−Rh arrangement. In agreement with this observation, an EHT study at different values for the P−Rh−P angle of the model complex **6** shows there is a very flat potential for the pivoting movement of the phosphine ligand around the rhodium atom (as little as 3 kcal/mol is necessary to drive the phosphine 45° out of linearity). Thus, as seen in the molecular structure of complex **4**, the distortion seems to result from steric interactions between the phosphine and the vinylidene ligands.

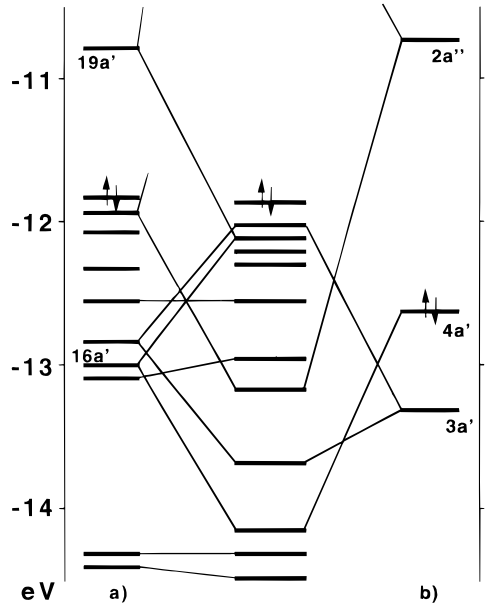

Figure 5. Molecular orbital diagram of complex $[Rh_2(\mu\text{-OOCH})(\mu\text{-}\sigma,\sigma\text{-C=CH}_2)(CO)_2(PH_3)_2]^+$ (**6**) (center) showing the interaction of ligand C=CH_2 (a) with fragment $[Rh_2(\mu\text{-OOCH})(CO)_2(PH_3)_2]^+$ (b).

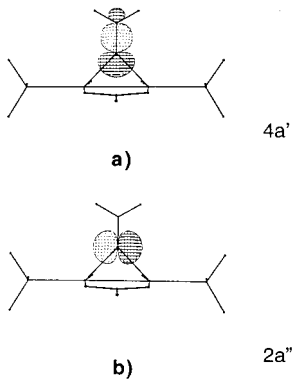

Figure 6. Some of the fragment orbitals of ligand $\mu\text{-}\sigma,\sigma$-C=CH_2 in model complex $[Rh_2(\mu\text{-OOCH})(\mu\text{-}\sigma,\sigma\text{-C=CH}_2)(CO)_2(PH_3)_2]^+$ (**6**): σ donor 4a′ (a); π acceptor 2a″(b).

Concluding Remarks

We have revealed that the terminal alkynols are useful starting materials, not only to prepare mononuclear allenylidene complexes but also to obtain homobimetallic μ-σ,σ-allenylidene compounds. Thus, we show the reaction of $[Rh(\mu\text{-}OOCCH_3)(CO)(PCy_3)]_2$ with 1,1-diphenyl-2-propyn-1-ol leads to $[Rh_2(\mu\text{-}OOCCH_3)(\mu\text{-}\eta^1{:}\eta^2\text{-}C_2C(OH)Ph_2)(CO)_2(PCy_3)_2]$, which affords $[Rh_2(\mu\text{-}OOCCH_3)(\mu\text{-}\sigma,\sigma\text{-}C{=}C{=}CPh_2)(CO)_2(PCy_3)_2]BF_4$ by protonation with $HBF_4{\cdot}OEt_2$. This complex is the first cationic μ-σ,σ-allenylidene derivative of this type for a group nine metal compound that is coordinatively unsaturated (30 valence electrons according to the EAN rule) and fully structurally characterized.

The X-ray structural characterization of $Rh_2(\mu\text{-}OOCCH_3)(\mu\text{-}\sigma,\sigma\text{-}C{=}C{=}CPh_2)(CO)_2(PCy_3)_2]BF_4$ shows a rhodium−rhodium distance in agreement with a single bond. EHT-MO calculations on the model cation confirm this metal−metal bond order and rationalize the valence electron count. They show a net acceptor behavior for the unsaturated η^1-carbon ligand and reveal the electronic nature, suggesting nucleophilic attack at the ligand is unlikely.

Experimental Section

General Considerations. All reactions were carried out under an argon atmosphere using Schlenk tube techniques. Solvents were dried and purified by known procedures and distilled under argon prior to use. 1,1-Diphenyl-2-propyn-1-ol was recrystallized from *n*-pentane. The starting complex $[Rh(\mu\text{-}OOCCH_3)(CO)(PCy_3)]_2$ (**1**) was prepared by a published method.[9] Elemental analyses were performed with a Perkin-Elmer 240 XL microanalyzer. NMR spectra were recorded on Varian UNITY 300 or Bruker AXR 300 instruments. Chemical shifts are expressed in parts per million, upfield from $Si(CH_3)_4$ ($^{13}C\{^1H\}$, ^1H) and 85% H_3PO_4 ($^{31}P\{^1H\}$). Infrared spectra were obtained from a Perkin-Elmer 783 instrument as Nujol mulls on polyethylene sheets or in solution using NaCl cells.

Preparation of $[Rh_2(\mu\text{-}OOCCH_3)(\mu\text{-}\eta^1{:}\eta^2\text{-}C_2C(OH)Ph_2)(CO)_2(PCy_3)_2]$ (2). A suspension of **1** (100 mg, 0.106 mmol) in *n*-pentane (20 mL) was treated with 1,1-diphenyl-2-propyn-1-ol (0.024 g, 0.116 mmol). The mixture was stirred for 2 h and changed from the original yellow suspension to a clear green solution. The volume was reduced to ca. 3 mL and cooled in dry ice to give a dark green microcrystalline solid. The solvent was decanted and the product washed several times with cold pentane. The crystals contain 1 mol of pentane/mol of **2**. Yield: 94 mg (82%). Anal. Calcd for $C_{55}H_{80}O_5P_2Rh_2{\cdot}C_5H_{12}$: C, 62.08; H, 7.93. Found: C, 61.94; H, 7.77. IR (pentane, cm^{-1}): ν(CO) 1985. IR (Nujol, cm^{-1}): $\nu(OCO_{asym})$ 1554, $\nu(OCO_{sym})$ 1442. ^1H NMR (300 MHz, $CDCl_3$, 20 °C, δ): 7.8−7.0 (m, 10 H, Ph); 3.69 (s, 1 H, O*H*); 1.77 (s, 3H, CH_3); 2.0−1.0 (m, 33H, C_6H_{11}). $^{13}C\{^1H\}$ NMR (75.45 MHz, $CDCl_3$, −30 °C, δ): 190.6 (dd, J_{Rh-C} = 75 Hz, J_{P-C} = 18 Hz, *C*O); 181.96 (s, O_2CCH_3); 128.3 (s, Ph); 127.6 (s, Ph); 126.5 (s, Ph); 111.2 (br, C_α); 99.3 (br, C_β); 76.12 (s, ≡*C*Ph_2OH); 34.3 (d, J_{P-C} = 33 Hz, CH_2CHP); 30.3 (d, $OCCCH_3$); 28.2 (d, J_{Rh-C} = 19.5 Hz, *C*H_2CHP); 26.9 (s, *C*H_2). $^{31}P\{^1H\}$ NMR (121.45 MHz, $CDCl_3$, 20 °C, δ): 44.1 (d, J_{Rh-P} = 147 Hz).

Preparation of $[Rh_2(\mu\text{-}OOCCH_3)(\mu\text{-}\sigma,\sigma\text{-}C{=}C{=}CPh_2)(CO)_2(PCy_3)_2]BF_4$ (3). A solution of **2** (150 mg, 0.14 mmol) in diethyl ether (20 mL) was treated with $HBF_4{\cdot}OEt_2$ (10 μl, 0.14 mmol). The color of the solution immediately turned from green to dark violet, and a solid precipitated from the solution. The mixture was stirred for 0.5 h and the volume reduced to ca. 5 mL. The solvent was decanted and the solid washed several times with diethyl ether and dried under vacuum. Recrystallization from dichloromethane/diethyl ether gave dark violet crystals. Yield: 126 mg (78%). Anal. Calcd for $C_{55}H_{68}BF_4O_4P_2Rh_2{\cdot}{}^1/_2CH_2Cl_2$: C, 55.48; H, 6.66. Found: C, 55.10; H, 6.79. IR (Nujol, cm^{-1}): ν(CO) 2026, 1995; ν(C=C=C) 1914; $\nu(OCO_{asym})$ 1538, $\nu(OCO_{sym})$ 1440; $\nu(BF_4)$ 1054. ^1H NMR (300 MHz, $CDCl_3$, 20 °C, δ): 7.8−7.2 (m, 10 H, Ph); 1.9 (s, 3H, CH_3); 2.2−1.2 (m, 33H, C_6H_{11}). $^{13}C\{^1H\}$ NMR (75.45 MHz, $CDCl_3$, 20 °C, δ): 186.9 (AA′MM′XX′ system, $^1J_{Rh-C}$ = 74 Hz; $^2J_{Rh-C}$ = 2.2 Hz; $^2J_{P-C}$ = 13.5 Hz); 186.2 (s, O*C*O); 181.3 (m, $^2J_{Rh-C}$ = 6 Hz, C_β); 174.2 (tt, $^2J_{Rh-C}$ = 52 Hz; $^2J_{P-C}$ = 36 Hz; C_α); 140.6 (d, J_{P-C} = 61.4 Hz, $C_{ipso-Ph}$); 134.2 (s, C_γ); 130.0 (d, $C_{para-Ph}$); 129.2 (2d, $C_{ortho-Ph}$, $C_{meta-Ph}$); 34.4 (d, CH_2CHP); 30.1 (s, CH_2CHP); 27.3(d, CH_2CHP); 25.8 (s, CH_2), 23.3 (s, CH_3). $^{31}P\{^1H\}$ NMR (121.45 MHz, $CDCl_3$, 20 °C, δ): 47.7 (AA′XX′ system, $J_{P-P'}$ = 9 Hz, J_{P-Rh} = 134 Hz, $J_{P-Rh'}$ = 116 Hz).

X-ray Structure Analysis of $C_{55}H_{79}BF_4O_4P_2Rh_2{\cdot}0.5CH_2Cl_2$ (3). A summary of crystal data and refinement parameters is reported in Table 3. Crystals suitable for the X-ray diffraction study were obtained from a dichloromethane/ether solution. An oil-coated rapidly cooled deep violet crystalline rectangular block of approximate dimensions 0.60 × 0.42 × 0.40 mm was mounted onto the tip of a glass fiber directly from solution.[19] A set of randomly searched reflections were indexed to monoclinic symmetry and accurate unit cell dimensions determined by least-squares refinement of 24 carefully centred reflections ($25 \le 2\theta \le 30$). Data were collected on a Siemens P4 diffractometer, with graphite-monochromated Mo Kα radiation by the $2\theta/\omega$ scan method. Three orientation and intensity standards were monitored every 55 min of measuring time throughout data collection; no variation was observed. Data were corrected for Lorentz and polarization effects, and for absorption using DIFABS.[20] The structure was solved by direct methods (SHELXTL PLUS)[21] and conventional Fourier techniques and refined by full-matrix least-squares on F^2 (SHELXL-93);[22] see Table 3. All non-hydrogen atoms were refined anisotropically except fluorine atoms of the BF_4 counterion. All hydrogens were included in fixed idealized positions. Half a solvent molecule of dichloromethene was located in the asymmetric unit. The Flack parameter was refined to −0.16(5), indicating the correct absolute structure determination. The largest peak and hole in the final difference map were measured as 2.245 and −0.797 e$Å^{-3}$.

Table 3. Crystallographic Data for Complex 3

formula	$C_{55}H_{79}BF_4O_4P_2Rh_2{\cdot}0.5(CH_2Cl_2)$
mol wt	1201.21
a, Å	12.802(3)
b, Å	17.560(5)
c, Å	13.726(3)
β, deg	97.66(1)
V, $Å^3$	3058.1(13)
cryst syst	monoclinic
space group	$P2_1$
Z	2
temp, °C	−100.0(2)
scan method	$\omega/2\theta$
θ (min−max), deg	1.5−25
octants	$-h,-k,\pm l$; $+h,+k,\pm l$
no. measd refls	11 725
no. indep refls	10 046
no. of params	611
GOOF	0.962
λ, Å	0.710 73
ρ_{calcd}, g cm^{-1}	1.305
μ, mm^{-1}	0.687
F(000)	1246
R(int)	0.0583
$R_1{}^a$	0.0616
$wR_2{}^a$	0.1979

(19) Kottke, T.; Stalke, D. *J. Appl. Crystallogr.* **1993**, *26*, 615.

(20) Walker, N.; Stuart, D. *Acta Crystallogr.* **1983**, *A39*, 1581.

(21) Sheldrick, G. M. SHELXTL PLUS. Siemens Analytical X-ray Instruments, Inc., Madison, WI, 1990.

(22) Sheldrick, G. M. SHELXL-93, Göttingen, Germany, 1993.

Acknowledgment. We thank the DGICYT (Projects PB96-0806 and PB94-1186, Programa de Promoción General del Conocimiento) and the EU (Project: Selective Processes and Catalysis Involving Small Molecules) for financial support. A.J.E. and J.S. thank the EU (Human, Capital and Mobility programme, CT93-0347) for grants.

Appendix

The extended Hückel calculations have been carried out on model complexes $[Rh_2(\mu\text{-}OOCH)(\mu\text{-}\sigma,\sigma\text{-}C{=}C{=}CH_2)(CO)_2(PH_3)_2]^+$ and $[Rh_2(\mu\text{-}OOCH)(\mu\text{-}\sigma,\sigma\text{-}C{=}CH_2)(CO)_2(PH_3)_2]^+$ using standard geometrical parameters and an idealized C_S symmetry based in the experimental structure of complex **3** and assuming a perfect linear arrangement for the P−Rh−Rh−P atoms. The calculations have been performed using the program CACAO[23] with the supplied atomic H_{ii} parameters.

Supporting Information Available: Tables of bond lengths and angles, anisotropic thermal parameters, and complete atomic coordinates and isotropic thermal parameters (8 pages). Ordering information is given on any current masthead page.

OM960164H

(23) Mealli, C.; Proserpio, D. M. *J. Chem. Educ.* **1990,** *67*, 39.